Title
Amyloid involvement in subcortical regions predicts cognitive decline

Journal
European Journal of Nuclear Medicine and Molecular Imaging, 45(13)

ISSN
1619-7070

Authors
Cho, Soo Hyun
Shin, Jeong-Hyeon
Jang, Hyemin
et al.

Publication Date
2018-12-01

DOI
10.1007/s00259-018-4081-5

Peer reviewed

HHS Public Access

Author manuscript

Eur J Nucl Med Mol Imaging. Author manuscript; available in PMC 2019 December 01.

Published in final edited form as:

Eur J Nucl Med Mol Imaging. 2018 December ; 45(13): 2368–2376. doi:10.1007/s00259-018-4081-5.

Amyloid involvement in subcortical regions predicts cognitive decline

Soo Hyun Cho[#1,2], **Jeong-Hyeon Shin**[#3], **Hyemin Jang**[1,2], **Seongbeom Park**[1,2], **Hee Jin Kim**[1,2], **Si Eun Kim**[1,2], **Seung Joo Kim**[1,2], **Yeshin Kim**[1,2], **Jin San Lee**[4], **Duk L. Na**[1,2,5,6], **Samuel N. Lockhart**[7], **Gil D. Rabinovici**[8], **Joon-Kyung Seong**[#3], **Sang Won Seo**[#1,2,6,9], and **Alzheimer's Disease Neuroimaging Initiative**

[1]Department of Neurology, Samsung Medical Center, Sungkyunkwan University School of Medicine, 81 Irwon-ro, Gangnam-gu, Seoul, 06351 Republic of Korea

[2]Neuroscience Center, Samsung Medical Center, Seoul, South Korea

[3]School of Biomedical Engineering, Korea University, Seoul, Republic of Korea

[4]Department of Neurology, Kyung Hee University Hospital, Seoul, South Korea

[5]Stem Cell & Regenerative Medicine Institute, Samsung Medical Center, Seoul, South Korea

[6]Department of Health Sciences and Technology, SAIHST, Sungkyunkwan University, Seoul, South Korea

[7]Internal Medicine - Gerontology and Geriatric Medicine, Wake Forest School of Medicine, Winston-Salem, NC, 27101 USA

[8]Memory and Aging Center, Department of Neurology, University of California, San Francisco, CA, USA

[9]Department of Clinical Research Design & Evaluation, SAIHST, Sungkyunkwan University, Seoul, South Korea

[#] These authors contributed equally to this work.

Abstract

Joon-Kyung Seong, Phone: +82-2-3290-5660, jkseong@korea.ac.kr. Sang Won Seo, Phone: +82-2-3410-1233, sangwonseo@empal.com.

Author contributions

S.H.C., J.H.S., J.K.S. and S.W.S. contributed to the conceptualization of the study, analysis and interpretation of data, and drafting. J.H.S. and S.P contributed to analyses of imaging data, prepared the figures, and provided technical support. H.J.K., H.M.J., S.E.K., S.J.K., Y.K. and J.S.L. contributed to interpretation of data. S.L., G.D.R. and D.L.N. contributed to analysis and interpretation of data.

Compliance with ethical standards

Conflict of interest All authors have no conflicts of interest to disclose.

Ethical approval All procedures performed in studies involving human participants were in accordance with the ethical standards of the institutional and/or national research committee and with the 1964 Helsinki declaration and its later amendments or comparable ethical standards.

Informed consent Informed consent was obtained from all individual participants included in the study.

Electronic supplementary material

ESM 1

(DOCX 334 kb) The letters marked in red in supplement are the part added while revision. I'd like you to change it to black when you publish it.

Purpose—We estimated whether amyloid involvement in subcortical regions may predict cognitive impairment, and established an amyloid staging scheme based on degree of subcortical amyloid involvement.

Methods—Data from 240 cognitively normal older individuals, 393 participants with mild cognitive impairment, and 126 participants with Alzheimer disease were acquired at Alzheimer's Disease Neuroimaging Initiative sites. To assess subcortical involvement, we analyzed amyloid deposition in amygdala, putamen, and caudate nucleus. We staged participants into a 3-stage model based on cortical and subcortical amyloid involvement: 382 with no cortical or subcortical involvement as stage 0, 165 with cortical but no subcortical involvement as stage 1, and 203 with both cortical and subcortical involvement as stage 2.

Results—Amyloid accumulation was first observed in cortical regions and spread down to the putamen, caudate nucleus, and amygdala. In longitudinal analysis, changes in MMSE, ADAS-cog 13, FDG PET SUVR, and hippocampal volumes were steepest in stage 2 followed by stage 1 then stage 0 (p value <0.001). Stage 2 showed steeper changes in MMSE score (β [SE] = −0.02 [0.004], $p < 0.001$), ADAS-cog 13 (0.05 [0.01], $p < 0.001$), FDG PET SUVR (−0.0008 [0.0003], $p = 0.004$), and hippocampal volumes (−4.46 [0.65], $p < 0.001$) compared to stage 1.

Conclusions—We demonstrated a downward spreading pattern of amyloid, suggesting that amyloid accumulates first in neocortex followed by subcortical structures. Furthermore, our new finding suggested that an amyloid staging scheme based on subcortical involvement might reveal how differential regional accumulation of amyloid affects cognitive decline through functional and structural changes of the brain.

Keywords

Amyloid staging; Amyloid PET; Alzheimer's dementia; Thal staging

Introduction

Amyloid-β protein (Aβ) deposition is one of the hallmarks of Alzheimer's disease (AD). Amyloid positron emission tomography (PET) is an established method for biomarker-supported diagnosis of AD and is now widely used [1]; it is now a valid tool for supporting a diagnosis of not only clinical but also preclinical AD [2]. Until now, a widely used method of quantifying amyloid load has been to estimate uptake in a target cortical region on PET, and using a threshold as a means of interpreting positivity. However, this amyloid PET approach may not properly utilize the full amount of regional information available.

According to pathological Aβ Thal staging [3], the deposition of Aβ plaques starts in the neocortex (phase 1) and limbic area (phase 2), then extends down into subcortical structures (striatum and amygdala, phase 3), brainstem (phase 4) and cerebellum (phase 5). In pathologic studies, presence of amyloid plaques in the striatum predicts higher Braak neurofibrillary tangle stage [4] and greater prevalence of dementia and clinicopathological AD [5, 6]. The presence of striatal plaques was also correlated with lower scores on several neuropsychological tests assessing memory [7].

Until now, it was unknown whether amyloid PET uptake [8] might also show the Aβ spreading pattern defined by neuropathology. In particular, previous studies suggest that there are methodological difficulties in using PET to conduct amyloid staging in vivo according to the pathologic amyloid staging criteria. Specifically, increased uptake in the hippocampus corresponding to Thal 2 is hard to detect, because prominent atrophy in AD patients can hinder proper quantification [8]. The brainstem and cerebellum, corresponding to Thal 4 and 5, have also been widely used as reference regions for analyzing target amyloid uptake. Furthermore, compared to cortical regions, subcortical regions corresponding to Thal 3 have a more diffuse form of amyloid plaques [3] which might present differently on in vivo Aβ PET imaging [9].

Recently, advances in neuroimaging techniques have enabled the delineation of human subcortical structures from T1-weighted MR images, and this morphometric analysis has been successfully employed in AD [10, 11, 12]. Moreover, surfacebased 3D modeling of subcortical structures makes it possible to investigate local atrophy in human subcortical structures, including thalamus, caudate nucleus, putamen, amygdala, globus pallidus, and hippocampus [13, 14]. When MR measures like surface-based segmentation of subcortical structures are aligned with amyloid PET images, they can enable the measurement of Aβ deposition more sensitively, which can lead to more accurate analysis of subcortical regional amyloid involvement in vivo.

In the present study, we investigated the spreading order of amyloid based on involvement in subcortical structures, and the effects of amyloid spread on clinical outcomes. We hypothesized that amyloid imaging would show increased amyloid uptake first in neocortex, then followed by subcortical structures including amygdala and striatum, following an in vivo staging scheme similar to pathological Aβ Thal phase. We further hypothesized that in vivo amyloid staging based on subcortical involvement would be reflective of not only structural and functional disease progression, measured by hippocampal atrophy and FDG hypometabolism, but also clinical deterioration, measured by MMSE and ADAS-Cog13, both cross-sectionally and longitudinally.

Materials and methods

Participants

All data used in the present study were obtained from the Alzheimer's Disease Neuroimaging Initiative (ADNI). ADNI is a multisite longitudinal biomarker study that has enrolled cognitively normal (CN) older individuals, people with amnestic mild cognitive impairment (MCI), and people with early AD (www.adni-info.org). The present study consisted of a total of 759 participants enrolled in the ADNI-1, ADNI-GO and ADNI-2 cohorts, who had concurrent ^{18}F-AV45 (Florbetapir) PET for assessing Aβ deposition and structural magnetic resonance imaging (MRI) scans available. Neuropsychological test scores (MMSE and ADAS13) from the same year as MRI examinations were used for cross-sectional analysis. The sample included 240 CN older individuals, 393 patients with MCI, and 126 patients with AD dementia. Detailed diagnostic criteria have been reported previously [15] and are published on the ADNI website (adni.loni.usc.edu/methods/). The

participants were followed up for 132 months in MMSE, 120 months in ADAS13, 96 months in FDG PET, and 120 months in Hippocampal volumes.

This study was approved by the Institutional Review Boards of all of the participating institutions. Informed written consent was obtained from all participants at each ADNI site.

MRI data acquisition

We downloaded MRI data from ADNI's databank as of September 2016, and available final MRI data included 759 patients. We used maximally-preprocessed 3-dimensional T1 magnetization-prepared rapid acquisition gradient echo (MPRAGE) MRI scans that have been corrected for non-uniformity and distortion, and at uniform voxel resolution. We used the MPRAGE that was closest in time to and within 3 months of the florbetapir scan. T1-MR images from 759 ADNI subjects were analyzed using FreeSurfer (v.5.1.0) for preprocessing. We downloaded hippocampal volume (HV) data from the ADNI website; HV was measured by semi-automated hippocampal volumetry carried out using a commercially available high dimensional brain mapping tool (Medtronic Surgical Navigation Technologies, Louisville, CO), that has previously been validated and compared to manual tracing of the hippocampus [16].

PET imaging analyses

Florbetapir images consisted of 4 × 5 min frames acquired at 50–70 min post injection; these were realigned, averaged, resliced to a common voxel size (1.5 mm × 1.5 mm × 1.5 mm), and smoothed to a common resolution of 8 mm^3. MPRAGE images that were acquired concurrently with the baseline florbetapir images were used as a structural template to define cortical and reference regions in native space for each subject using FreeSurfer. We downloaded FDG PET data from the ADNI website. These were subject averages (using 30–60 min FDG SUVR data) from a set of pre-defined regions of interest (ROIs) cited frequently in FDG-PET studies of AD and MCI patients [17]. This metaROI included angular, temporal, and posterior cingulate ROIs. MetaROI means were normalized by dividing by each subject's pons/vermis reference region mean.

Image processing steps

We constructed both cortical and subcortical surface meshes from T1 images of each subject similarly to our previous work [13, 18]. Both surface meshes were registered to the template meshes in order to provide vertex correspondences across the sample [18, 19]. For measuring standardized uptake value ratios (SUVR) from PET images, each florbetapir image was co-registered to the T1 image using affine coregistration (FSL-FLIRT). Finally, SUVR values (normalized by mean uptake of cerebellar cortex) acquired from each subject's florbetapir PET image were assigned to each vertex of the cortical and subcortical surface meshes.

Determination of spreading order for amyloid

For selecting the control data, amyloid positivity was defined as a florbetapir-PET cortical SUVR >1.11 [20]; for assessing the regional involvement of amyloid, we used a Z score cutoff as suggested by a recent paper [8]. Note that the cutoff value of 1.11 was only used

for determining global amyloid positivity. With this criterion, we selected 156 amyloid-negative cognitively normal controls; these were used for calculating regional Z scores. For all participants, regional Z scores of amyloid PET were calculated for cortical and subcortical regions.

To determine the order of spreading, we assumed that regions with earlier-appearing pathology would show increased binding in a greater number of participants, with regional amyloid involvement defined as a Z score value >1.5. First, we sorted seven regions (global cortex, putamen, caudate, amygdala, thalamus, hippocampus and pallidum) in descending order by the number of participants whose regional Z score values were > 1.5 for each region. In addition, participants were staged by the degree of regional involvement.

To assess differences in regional involvement frequency across these regions, we used a bootstrapping method with 1000 resamples in R v3.4.1 (Institute for Statistics and Mathematics, Vienna, Austria; www.R-project.org) to derive the estimates of 95% confidence intervals and standard error. For all combinations of regional pairs, asymptotic p-values were calculated and were corrected for multiple comparisons with Bonferroni's method to control increasing type I errors.

Image-based staging of amyloid PET

After determination of the spreading order of amyloid pathology, we selected three subcortical regions (caudate nucleus, putamen and amygdala) which start to accumulate amyloid plaque in Thal phase 3 [3]. We defined cortical amyloid positivity when the cortical Z score was >1.5 and defined subcortical amyloid positivity when the Z score was >1.5 in at least two of the three subcortical regions. Based on cortical and subcortical amyloid deposition, we classified participants into three staging groups: no involvement in cortical or subcortical regions (stage 0), cortical involvement without subcortical involvement (stage 1) and involvement in both cortical and subcortical regions (stage 2) (Fig. 1). A small number of unstageable participants were excluded from statistical analysis.

Statistical analyses

In order to compare demographic and clinical characteristics among diagnostic groups or among stages, we performed analysis of variance (ANOVA) for continuous variables and chi-square test for categorical variables. We performed analysis of covariance (ANCOVA) after controlling for age, sex and education to compare florbetapir PET and FDG PET SUVR and cognitive performance (MMSE and ADAS-Cog13) among the three amyloid stages (stage 0, 1 and 2). In order to compare hippocampal volumes among stages, we performed ANCOVA after controlling for age, sex, education and intracranial volume (ICV) among the three amyloid stages (stage 0, 1 and 2), and Bonferroni correction was performed with post hoc test.

In order to compare longitudinal cognitive decline and FDG PET SUVR among stages, linear mixed-effects models were performed after including age, sex, education, amyloid staging group, time (quantified as month from baseline visit), ICV (added in hippocampal volume analyses) and an amyloid staging group by time interaction as fixed effects along with participant-specific random effects.

In order to compare rates of conversion to dementia between MCI patients with stage 1 and those with stage 2, we performed cox regression after controlling for age, sex, and education.

We used Med Calc Statistical Software version 17.9.2 (Ostend, Belgium; 2017) for ANOVA and chi-square test, Stata software (Stata Corp. 2017. Stata Statistical Software: Release 15. College Station, TX: Stata Corp LLC) for linear mixed-effects models, and R v3.4.1 (Institute for Statistics and Mathematics, Vienna, Austria; www.R-project.org) for Kaplan-Meier and Cox regression.

Results

Demographic characteristics

Demographic characteristics of the participants are summarized in eTable 1. There was no difference in sex between the three diagnostic groups; however, age and education level was different across the groups. Frequency of APOEε4 carrier was 26.7% in CN, 43.6% in MCI and 66.4% in AD. Frequency of florbetapir positivity was 35.4% in CN, 53.7% in MCI and 86.5% in AD.

In vivo amyloid stages based on subcortical involvement

To examine the regional spreading order of amyloid, we investigated the regional frequencies of amyloid involvement (eTable 2). Amyloid accumulation showed a stepwise pattern, being most frequently observed in the cerebral cortex (38.4%), followed by the putamen (18.9%), caudate (15.5%), amygdala (8.5%), and then thalamus, hippocampus and pallidum (Fig. 2).

Based on cortical and subcortical involvement of amyloid, 759 participants were classified into three stages: 382 patients into stage 0, 165 patients into stage 1, and 203 patients into stage 2 (Fig. 1). Nine out of 759 participants (1.2%) with amyloid involvement in subcortical structures but lacking cortical involvement were classified as unstageable. Compared to stage 0, stage 1 and stage 2 were older and had more frequent APOEε4 genotype (Table 1).

Differences in baseline cognitive measures, FDG PET SUVR and hippocampal volumes among amyloid stages

We found differences in the proportion of diagnoses across in vivo amyloid stages, (χ^2 = 94.70, $p < .001$) (Table 1 and Fig. 3). In stage 2, there were more AD patients than in stage 1 ($\chi^2 = 52.88$, $p < 0.001$). MMSE score was lowest in stage 2 (mean ± SD, 26.1 ± 0.2), followed by stage 1 (26.9 ± 0.2) and then stage 0 (28.5 ± 0.1). ADAS-cog 13 was highest in stage 2 (21.2 ± 0.6) followed by stage 1 (17.6 ± 0.7) and then stage 0 (11.6 ± 0.5). FDG PET SUVR was lowest in stage 2 (1.18 ± 0.01), followed by stage 1 (1.22 ± 0.01) and then stage 0 (1.30 ± 0.01). Hippocampal volume was lowest in stage 2 (6594.0 ± 74.7), followed by stage 1 (6843.1 ± 87.0) and then stage 0 (7268.5 ± 55.2).

Longitudinal changes of cognitive measures, FDG PET SUVR and hippocampal volumes among amyloid stages

Decline in MMSE score was steepest in stage 2 (stage 2 X Time, β [SE] = −0.05 [0.004], p < 0.001), followed by stage 1 (stage 1 X Time β, [SE] = −0.04 [0.003], p < 0.001), then stage 0 (Fig. 4 and eTable 3). Incline in ADAS-cog 13 score increased steepest in stage 2 (β [SE] = 0.15 [0.008], p < 0.001), followed by stage 1 (β [SE] = 0.10 [0.008], p < 0.001), then stage 0. Decrease of FDG PET SUVR was steepest in stage 2 (β [SE] = −0.001 [0.0002], p < 0.001), followed by stage 1 (β [SE] = −0.0004 [0.0002], p = 0.13), then stage 0. Decrease of hippocampal volumes were steepest in stage 2 (β [SE] = −9.78 [0.53], p < 0.001), followed by stage 1 (β [SE] = −5.32 [0.56], p < 0.001), then stage 0.Compared to stage 1, stage 2 showed steeper changes in MMSE score (β [SE] = −0.02 [0.004], p < 0.001), ADAS-cog 13 (β [SE] = 0.05 [0.01], p < 0.001), FDG PET SUVR (β [SE] = −0.0008 [0.0003], p = 0.004), and hippocampal volumes (β [SE] = −4.46 [0.65], p < 0.001).

We additionally performed sensitivity analyses according to various cutoffs and numbers of subcortical structures involved in defining subcortical amyloid positivity (eTable 4). We examined differences in cognitive dysfunction or decline among amyloid stages and found that results were similar regardless of cutoff or number of structures used to define subcortical positivity.

Conversion ratio to dementia in MCI patients

Among 180 MCI patients with stage 1 or 2 amyloid involvement, 67 patients (23 patients with stage 1 and 44 patients with stage 2) converted to dementia (Fig. 5). Cox regression showed that MCI patients with stage 2 had a higher risk of conversion to dementia throughout the observation period than those with stage 1 (HR: 2.07, 95% CI: 1.23–3.50).

Discussion

In the present study, we investigated the spreading pattern of amyloid based on involvement in subcortical structures, and the clinical effects of subcortical amyloid involvement using cross-sectional and longitudinal outcomes. First, we found that amyloid accumulated first in neocortex and then in subcortical structures, suggesting that amyloid has a downward spreading pattern. Second, even among amyloid-positive patients, those with subcortical involvement (stage 2) showed worse cognitive impairment than those without subcortical involvement (stage 1). Finally, patients with subcortical involvement (stage 2) revealed steeper cognitive decline compared to those without subcortical involvement (stage 1). Taken together, our findings suggest that in vivo amyloid imaging enables the staging of amyloid burden in living patients according to subcortical involvement, and that subcortical amyloid predicts worse clinical outcomes.

Our first major finding was that amyloid accumulated first in neocortex and then in subcortical structures, suggesting that amyloid has a downward spreading pattern. Previous studies suggest that there are methodological difficulties in using PET to conduct amyloid staging in vivo based on involvement of subcortical regions. However, our finding is in line with recent studies showing that in vivo amyloid staging was possible and that the striatum

was the last deposition region [21, 22]. In particular, we found that thalamus and pallidum, which are subcortical structures that are not part of Thal phase 3, were the last spreading regions of amyloid. Our staging strategy based on subcortical amyloid deposition also showed a highly consistent deposition pattern across participants, allowing us to classify 98.8% (750/759) of participants into any of the three successive amyloid stages. Therefore, the PET-measured amyloid deposition indicated a predictable regional sequence that enabled in vivo staging analogous to established neuropathologic approaches for staging amyloid.

Our second major finding was that even if patients were amyloid positive, patients with subcortical involvement (stage 2) showed worse cognitive impairment than those without subcortical involvement (stage 1). Specially, we found that AD patients were more commonly included in higher stages while cognitively normal individuals were more common in lower stages. Therefore, consistent with previous pathological studies, we showed that involvement of amyloid plaques both in cortical and subcortical structures is more strongly associated with presence of dementia [5, 23] or cognitive impairment [21] than amyloid in the cortex alone. Our findings suggest that subcortical amyloid deposition and a higher in vivo amyloid stage signify an advanced disease course. This could also be supported by a recent study with Parkinson's disease (PD) patients [24], which showed that in PD, the combined presence of striatal and cortical amyloid deposition is associated with greater cognitive impairment than cortical amyloidopathy alone.

Our final major finding was that longitudinal analyses revealed that patients with stage 2 amyloid involvement had steeper cognitive decline and functional and structural deterioration, indexed by FDG PET and hippocampal volumes, than stage 0 and 1 patients. There are several studies predicting faster decline in MCI or AD patients using imaging markers, including measures of amyloid, cortical thickness, hippocampal volume, and glucose hypometabolism [25, 26]. There have been recent reports that amyloid-positive people show more rapid cognitive decline [27, 28]. However, little research has been done to determine if fast decline can be predicted based on the distribution of amyloid among amyloid-positive participants. A recent work suggested that striatal involvement of amyloid predicted subsequent cognitive decline [22]. Additionally, we found that patients with subcortical involvement of amyloid had steeper functional and structural brain changes than those without subcortical involvement of amyloid. These results suggest that it is important to investigate subcortical amyloid involvement when interpreting amyloid PET.

The reason why subcortical amyloid pathology might be associated with more severe cognitive decline has not been extensively investigated. However, there are several possible hypotheses. In the present study, compared to patients without subcortical involvement (stage 1), patients with subcortical involvement (stage 2) showed more cortical amyloid burden, hypometabolism and hippocampal atrophy. Therefore, our results suggest that subcortical involvement of amyloid might affect cognitive decline through several processes, including greater cortical amyloid burden and functional and structural changes.

The present study has some limitations. First, we used a cutoff Z score of 1.5 to determine regional amyloid involvement, which may have affected our results; however, our sensitivity analyses (eTable 4) showed that similar results were obtained regardless of threshold used,

thus mitigating this limitation. Second, there were nine unstageable CN and MCI participants who showed subcortical amyloid involvement without cortical amyloid involvement, but this was only 1.2% of the sample. Previous studies of patients with certain presenilin-1 mutations [29] or amyloid precursor protein gene duplication showed predominantly striatal increases in [^{11}C] PIB uptake even in cognitively normal mutation carriers. More research should be done to understand these predominantly striatal patterns of amyloid deposition. Third, we could not include cerebellum among the staging regions because we used cerebellum as a reference region. Hippocampus was also not included in our amyloid staging scheme because hippocampal uptake can be prominently affected by atrophy and hard to detect. Fourth, we used a common regional cutoff value, but future research should investigate possible region-specific cutoffs for amyloid staging. Finally, our percentage of amyloid involvement in subcortical regions in CN participants (13.8%) seems to be higher than those reported by previous studies (7% [21] or 8% [22]). The percentage of amyloid negative AD (Stage 0；17.5%) seems to be slightly higher compared to those of previous studies (11% [21] or 12% [22]). This discrepancy might be related to differences in imaging analysis methods. However, we think that our analyses have an advantage in segmenting subcortical structures [18]. Specifically, the previous studies employed the volume-based segmentation methods, while in this study we applied a surface-based method to delineate the subcortical structures. Even with these limitations, by measuring subcortical amyloid SUVR, we can predict whether or not a patient is at an advanced point in the evolution of disease.

Conclusions

In vivo amyloid imaging enables us to stage amyloid burden in living patients according to degree of subcortical involvement, and subcortical involvement predicts worse clinical outcomes. Our findings suggest that, while cortical amyloid positivity is important, it is also important to consider subcortical amyloid involvement.

Supplementary Material

Refer to Web version on PubMed Central for supplementary material.

Funding

This research was supported by a National Research Foundation of Korea (NRF) grant funded by the Korean government (MSIP) (No. NRF-2017R1A2B2005081 and No. 2016R1A2B4014398) and National Institutes of Health (NIH) grant P30AG049638.

Role of the funder The funders had no role in the design and conduct of the study；collection, management, analysis, and interpretation of the data；preparation, review, or approval of the manuscript；or decision to submit the manuscript for publication.

References

1. Jack CR, Jr, Knopman DS, Jagust WJ, Petersen RC, Weiner MW, Aisen PS, et al. Tracking pathophysiological processes in Alzheimer’s disease: an updated hypothetical model of dynamic biomarkers. Lancet Neurol 2013;12:207–16. [PubMed: 23332364]

2. Jack CR, Jr, Knopman DS, Jagust WJ, Shaw LM, Aisen PS, Weiner MW, et al. Hypothetical model of dynamic biomarkers of the Alzheimer's pathological cascade. Lancet Neurol 2010;9:119–28. [PubMed: 20083042]
3. Thal DR, Rub U, Orantes M, Braak H. Phases of a beta-deposition in the human brain and its relevance for the development of AD. Neurology 2002;58:1791–800. [PubMed: 12084879]
4. Braak H, Braak E. Alzheimer's disease: striatal amyloid deposits and neurofibrillary changes. J Neuropathol Exp Neurol 1990;49:215–24. [PubMed: 1692337]
5. Beach TG, Sue LI, Walker DG, Sabbagh MN, Serrano G, Dugger BN, et al. Striatal amyloid plaque density predicts Braak neurofibrillary stage and clinicopathological Alzheimer's disease: implications for amyloid imaging. J Alzheimers Dis 2012;28:869–76. [PubMed: 22112552]
6. Thal DR, Beach TG, Zanette M, Heurling K, Chakrabarty A, Ismail A, et al. [(18)F]flutemetamol amyloid positron emission tomography in preclinical and symptomatic Alzheimer's disease: specific detection of advanced phases of amyloid-beta pathology. Alzheimers Dement 2015;11:975–85. [PubMed: 26141264]
7. Wolf DS, Gearing M, Snowdon DA, Mori H, Markesbery WR, Mirra SS. Progression of regional neuropathology in Alzheimer disease and normal elderly: findings from the Nun study. Alzheimer Dis Assoc Disord 1999;13:226–31. [PubMed: 10609672]
8. Cho H, Choi JY, Hwang MS, Kim YJ, Lee HM, Lee HS, et al. In vivo cortical spreading pattern of tau and amyloid in the Alzheimer disease spectrum. Ann Neurol 2016;80:247–58. [PubMed: 27323247]
9. Seo SW, Ayakta N, Grinberg LT, Villeneuve S, Lehmann M, Reed B, et al. Regional correlations between [11C]PIB PET and post-mortem burden of amyloid-beta pathology in a diverse neuropathological cohort. Neuroimage Clin 2017;13:130–7. [PubMed: 27981028]
10. Stepan-Buksakowska I, Szabo N, Horinek D, Toth E, Hort J, Warner J, et al. Cortical and subcortical atrophy in Alzheimer disease: parallel atrophy of thalamus and hippocampus. Alzheimer Dis Assoc Disord 2014;28:65–72. [PubMed: 23751371]
11. Ma X, Li Z, Jing B, Liu H, Li D, Li H, et al. Identify the atrophy of Alzheimer's disease, mild cognitive impairment and normal aging using morphometric MRI analysis. Front Aging Neurosci 2016;8:243. [PubMed: 27803665]
12. Doan NT, Engvig A, Zaske K, Persson K, Lund MJ, Kaufmann T, et al. Distinguishing early and late brain aging from the Alzheimer's disease spectrum: consistent morphological patterns across independent samples. Neuroimage 2017;158:282–95. [PubMed: 28666881]
13. Chung SJ, Shin JH, Cho KH, Lee Y, Sohn YH, Seong JK, et al. Subcortical shape analysis of progressive mild cognitive impairment in Parkinson's disease. Mov Disord 2017;32:1447–56. [PubMed: 28737237]
14. Koo DL, Shin JH, Lim JS, Seong JK, Joo EY. Changes in subcortical shape and cognitive function in patients with chronic insomnia. Sleep Med 2017;35:23–6. [PubMed: 28619178]
15. Petersen RC, Aisen PS, Beckett LA, Donohue MC, Gamst AC, Harvey DJ, et al. Alzheimer's disease neuroimaging initiative (ADNI): clinical characterization. Neurology 2010;74:201–9. [PubMed: 20042704]
16. Hsu YY, Schuff N, Du AT, Mark K, Zhu X, Hardin D, et al. Comparison of automated and manual MRI volumetry of hippocampus in normal aging and dementia. J Magn Reson Imaging 2002;16:305–10. [PubMed: 12205587]
17. Landau SM, Harvey D, Madison CM, Koeppe RA, Reiman EM, Foster NL, et al. Associations between cognitive, functional, and FDG-PET measures of decline in AD and MCI. Neurobiol Aging 2011;32:1207–18. [PubMed: 19660834]
18. Cho Y, Seong JK, Shin SY, Jeong Y, Kim JH, Qiu AQ, et al. A multi-resolution scheme for distortion-minimizing mapping between human subcortical structures based on geodesic construction on Riemannian manifolds. Neuroimage 2011;57:1376–92. [PubMed: 21658456]
19. Cho Y, Seong JK, Jeong Y, Shin SY. Alzheimer's disease neuroimaging I. Individual subject classification for Alzheimer's disease based on incremental learning using a spatial frequency representation of cortical thickness data. Neuroimage 2012;59:2217–30. [PubMed: 22008371]

20. Landau SM, Breault C, Joshi AD, Pontecorvo M, Mathis CA, Jagust WJ, et al. Amyloid-beta imaging with Pittsburgh compound B and florbetapir: comparing radiotracers and quantification methods. J Nucl Med 2013;54:70–7. [PubMed: 23166389]
21. Grothe MJ, Barthel H, Sepulcre J, Dyrba M, Sabri O, Teipel SJ. In vivo staging of regional amyloid deposition. Neurology 2017;89:2031–8. [PubMed: 29046362]
22. Hanseeuw BJ, Betensky RA, Mormino EC, Schultz AP, Sepulcre J, Becker JA, et al. PET staging of amyloidosis using striatum. Alzheimers Dement 2018.
23. Beach TG, Thal DR, Zanette M, Smith A, Buckley C. Detection of striatal amyloid plaques with [18F]flutemetamol: validation with postmortem histopathology. J Alzheimers Dis 2016;52:863–73. [PubMed: 27031469]
24. Shah N, Frey KA, Muller ML, Petrou M, Kotagal V, Koeppe RA, et al. Striatal and cortical beta-Amyloidopathy and cognition in Parkinson's disease. Mov Disord 2016;31:111–7. [PubMed: 26380951]
25. Dickerson BC, Wolk DA. Biomarker-based prediction of progression in MCI: comparison of AD signature and hippocampal volume with spinal fluid amyloid-β and tau. Front Aging Neurosci 2013;5.
26. Landau SM, Mintun MA, Joshi AD, Koeppe RA, Petersen RC, Aisen PS, et al. Amyloid deposition, hypometabolism, and longitudinal cognitive decline. Ann Neurol 2012;72:578–86. [PubMed: 23109153]
27. Okello A, Koivunen J, Edison P, Archer HA, Turkheimer FE, Nagren K, et al. Conversion of amyloid positive and negative MCI to AD over 3 years: an 11C-PIB PET study. Neurology 2009;73:754–60. [PubMed: 19587325]
28. Doraiswamy PM, Sperling RA, Johnson K, Reiman EM, Wong TZ, Sabbagh MN, et al. Florbetapir F 18 amyloid PET and 36-month cognitive decline: a prospective multicenter study. Mol Psychiatry 2014;19:1044–51. [PubMed: 24614494]
29. Klunk WE, Price JC, Mathis CA, Tsopelas ND, Lopresti BJ, Ziolko SK, et al. Amyloid deposition begins in the striatum of presenilin-1 mutation carriers from two unrelated pedigrees. J Neurosci 2007;27:6174–84. [PubMed: 17553989]

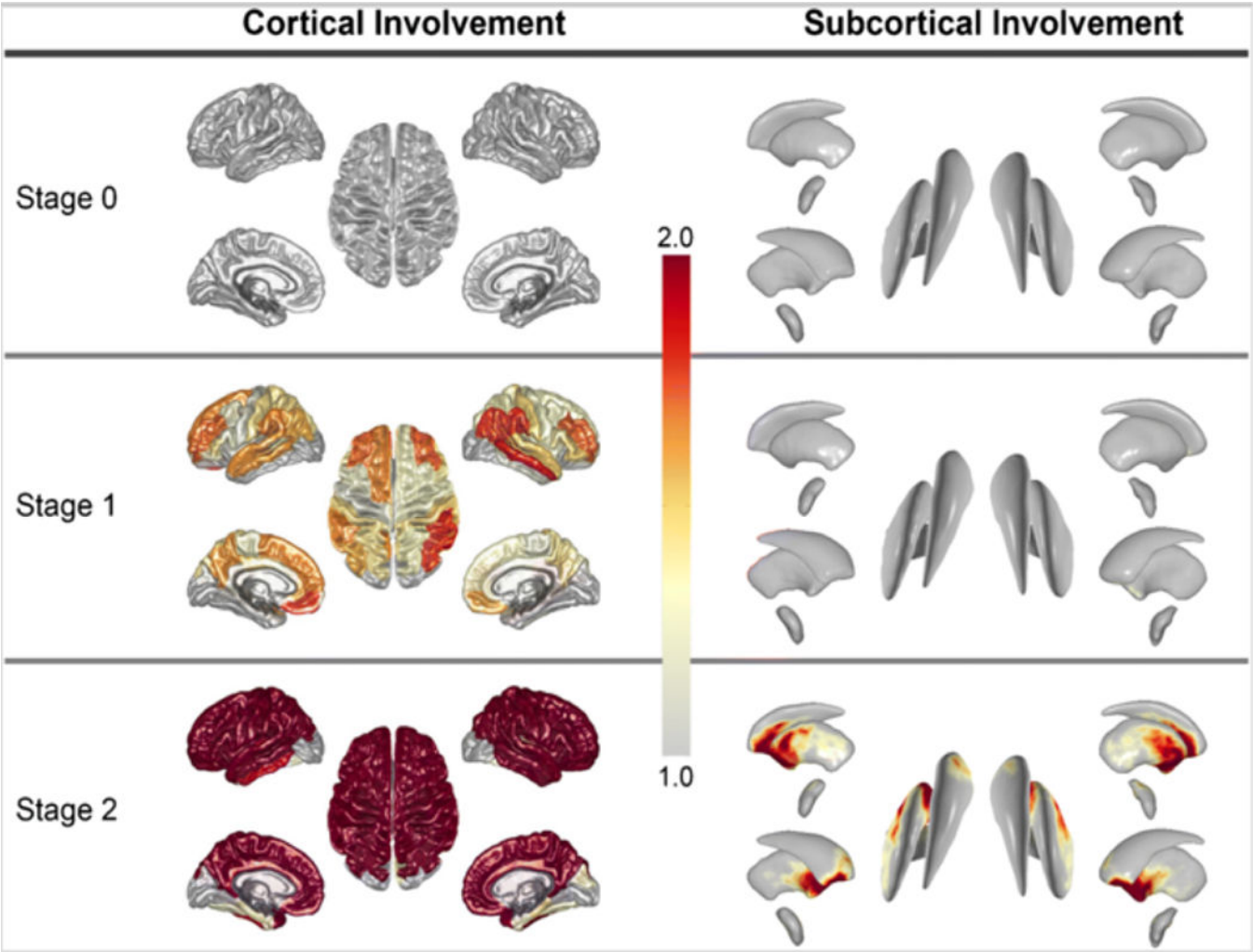

Fig. 1.

Cortical and subcortical regions with increased amyloid burden for each amyloid stage. This visualizes the surfacebased mapping of the average Z scores of the amyloid SUVRs for each stage. The surface mapping shows the regions with increased amyloid binding. Stage 0: no amyloid involvement in cortical or subcortical regions. Stage 1: cortical amyloid involvement without subcortical regional involvement. Stage 2: amyloid involvement in both cortical and subcortical regions

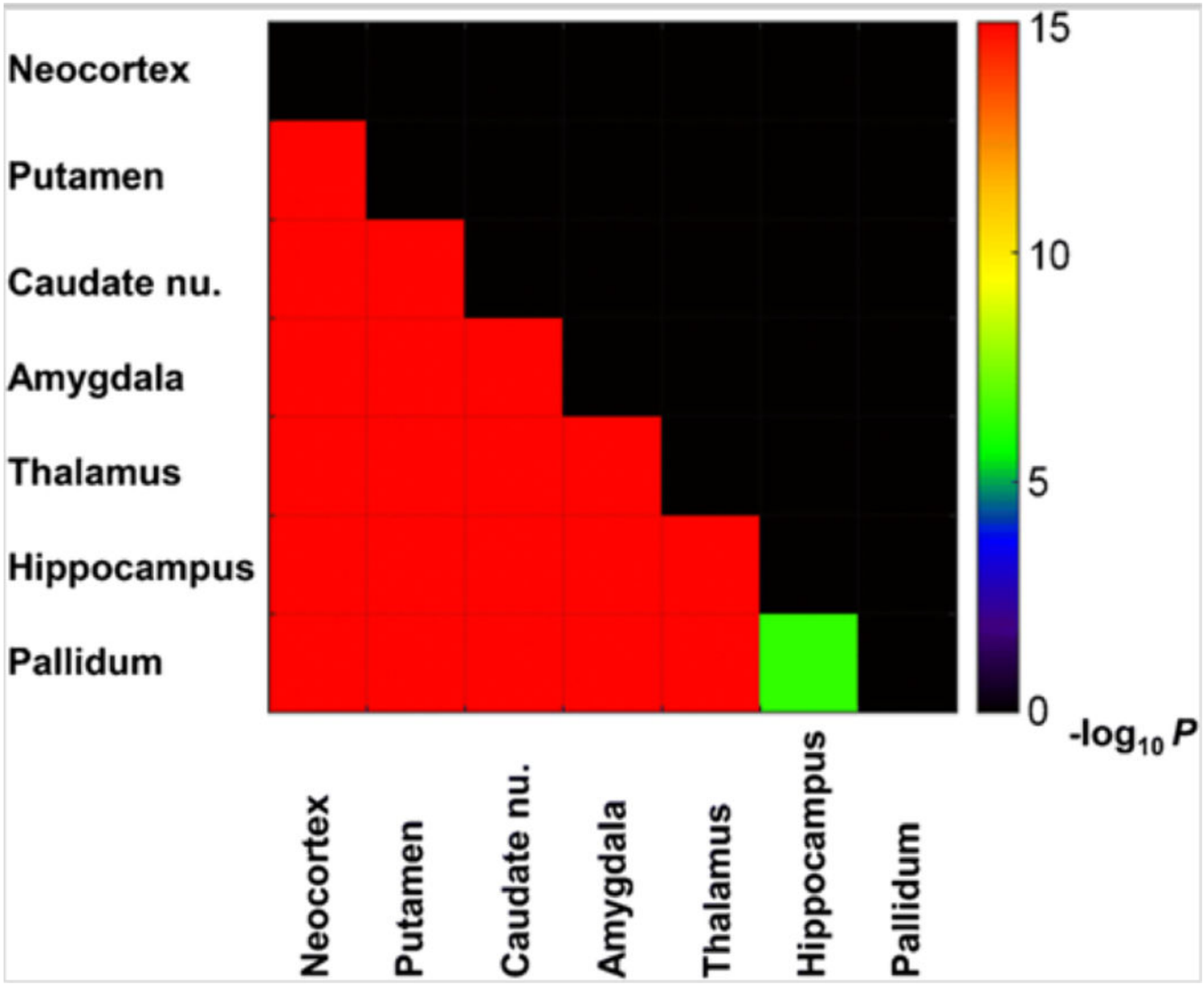

Fig. 2.

Colorcoded two dimensional heat maps. This map shows the statistical significance for the comparison of the frequencies of regional involvement between each pair of regions. The differences of regional involvement frequency of amyloid shows a stepwise pattern. There is a clear difference of the involvement frequency of amyloid in most pairs of neocortex and subcortical regions. Only the pairs of comparison passing Bonferroni's multiple comparisons are displayed. Color bars represent logarithmic scale of Pvalue ($-\log_{10}P$)

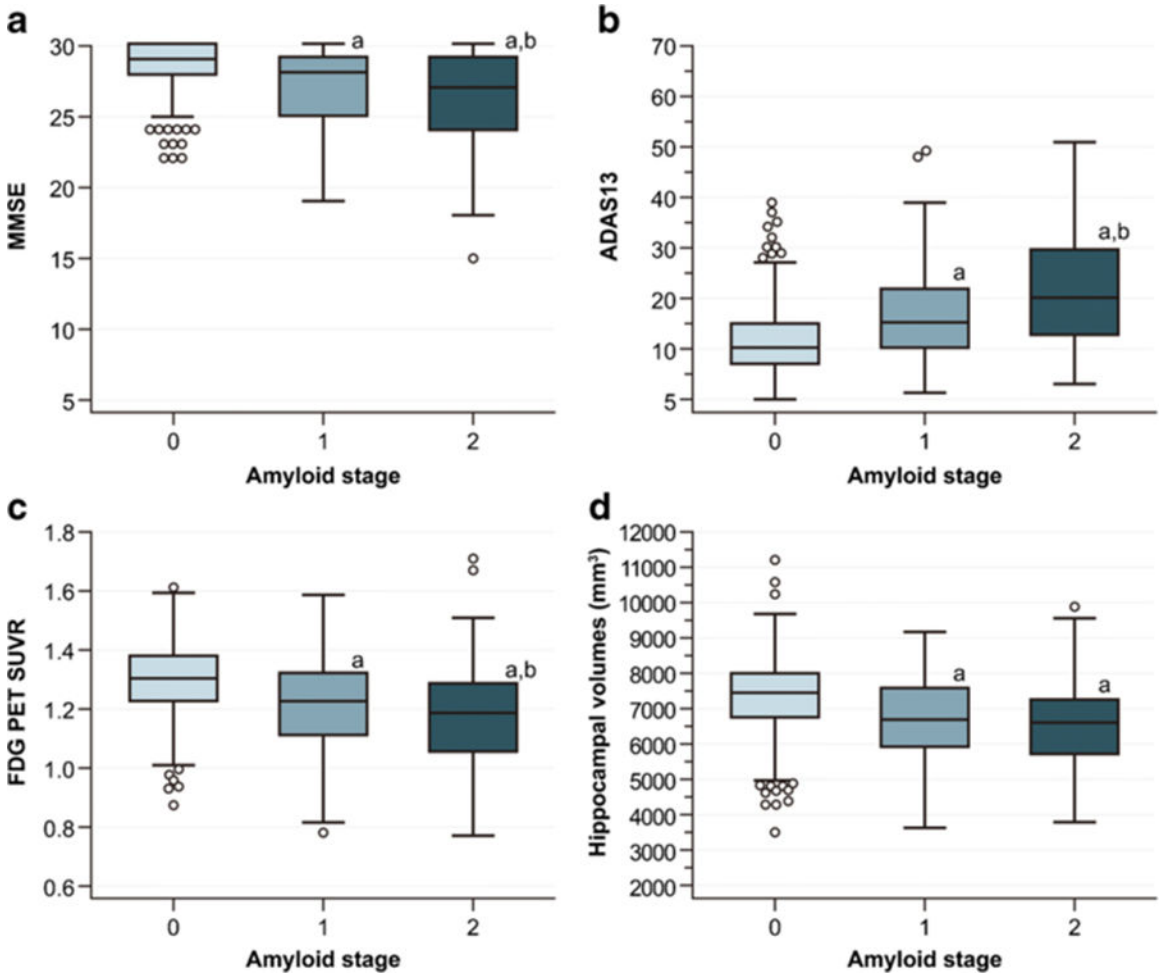

Fig. 3.

Comparison of cognitive measures, FDG PET SUVR and hippocampal volumes among the amyloid stages. (a) MMSE score was lowest in stage 2, followed by stage 1 and then stage 0. (b) ADAS-cog 13 was highest in stage 2 followed by stage 1 and then stage 0. (c) FDG PET SUVR was lowest in stage 2, followed by stage 1 and then stage 0. (d) Hippocampal volumes were lowest in stage 2, followed by stage 1 and then stage 0. P values for differences between stages are from analysis of covariance with covariates of age, sex and education for MMSE, ADAS13 and FDG PET SUVR, plus ICV for hippocampal volumes. Stage 0 means no amyloid involvement in cortical or subcortical regions. Stage 1 means cortical amyloid involvement without subcortical involvement. Stage 2 means amyloid involvement in both cortical and subcortical regions. [a] $p < 0.05$ in comparison between stage 0 and stage 1 or stage 2. [b] $p < 0.05$ in comparison between stage 1 and stage 2.
Abbreviations: MMSE, Mini-Mental State Examination; ADAS, Alzheimer's Disease Assessment Scale-cognitive subscale; ICV, Intracranial volume

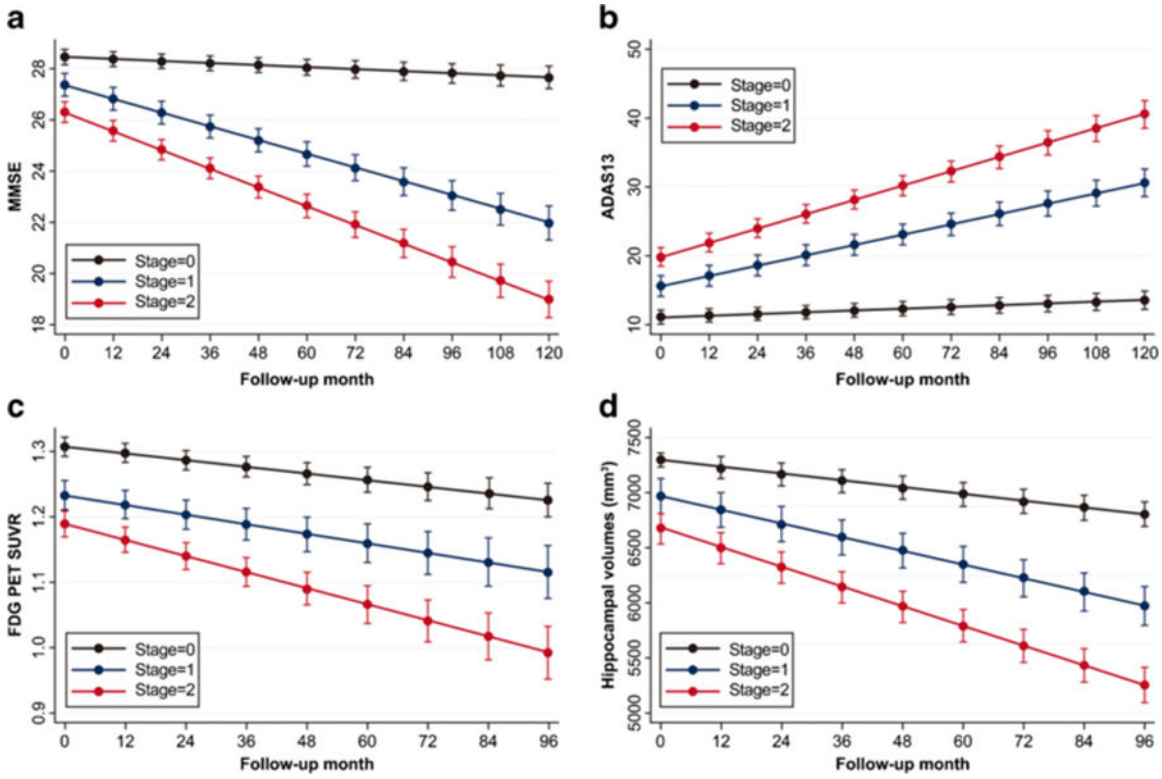

Fig. 4.

Longitudinal changes of cognitive measures FDG PET SUVR and hippocampal volumes among amyloid stages. (a) Decline in MMSE score was steepest in stage 2, followed by stage 1 and stage 0. (b) Incline in ADAS-cog 13 score was steepest in stage 2, followed by stage 1 and stage 0. (c) Decline in FDG PET SUVR was steepest in stage 2, followed by stage 1 and stage 0. (d) Decline in hippocampal volumes were steepest in stage 2, followed by stage 1 and stage 0. Linear mixed-effects models were performed after including age, sex, education, amyloid staging group, time (quantified as month from baseline visit), ICV (added in hippocampal volume analyses) and an amyloid staging group by time interaction as fixed effects along with participant-specific random effects. This is a graph plotting the mean of the predicted values for each follow up month derived from the predicted model equation using a linear mixed effect model. Error bars are 95% confidence intervals. Abbreviations: MMSE, Mini-Mental State Examination; ADAS, Alzheimer's Disease Assessment Scale-cognitive subscale; ICV, Intracranial volume

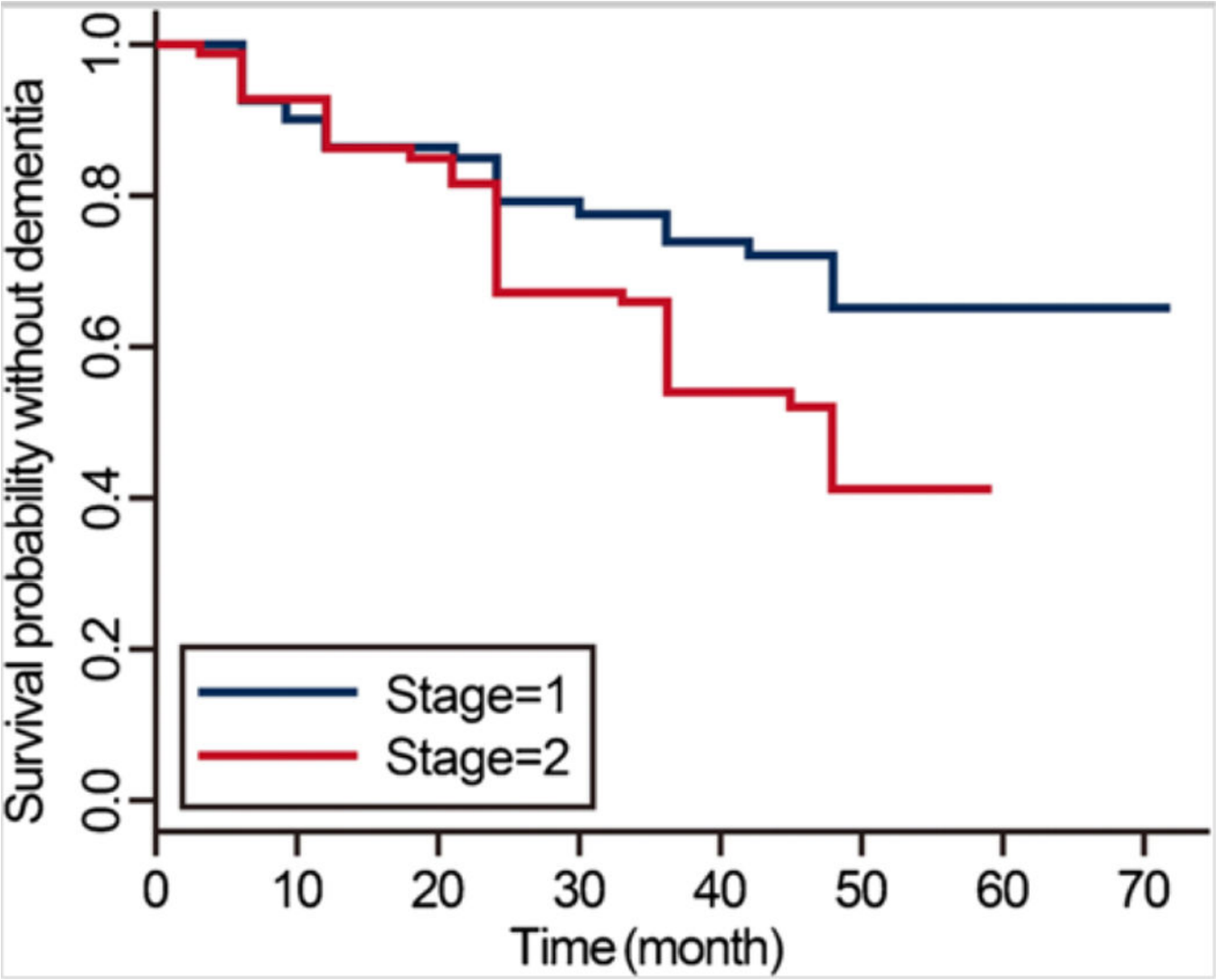

Fig. 5.

Kaplan-Meier survival curve of the time until conversion to dementia. Cox regression after controlling for age, sex, and education showed that MCI patients with stage 2 had a higher risk of conversion to dementia throughout the observation period than those with stage 1 (HR: 2.07, 95% CI: 1.23–3.50)

Table 1

Demographic and clinical characteristics according to amyloid staging group

Characteristic	Amyloid stage			
	0 (N = 382)	1 (N = 165)	2 (N = 203)	Unstageable (N = 9)
Age, years	71.0 (7.2)	74.5 (6.6)[a]	73.5 (7.2) [a]	70.7 (7.3)
Female sex, No. (%)	183 (47.9)	87 (52.7)	90 (44.3)	2 (22.2)
Education, y	16.5 (2.5)	16.0 (2.9)	16.2 (2.7)	17.6 (2.6)
APOEε4, No. (%)	83 (21.8)	93 (56.4)[a]	141 (69.8) [a,b]	1 (11.1)
Diagnosis[a]				
CN, No.(%, N = 240)	160 (66.7)	44 (18.3)[a]	33 (13.8)[a,b]	3 (1.3)
MCI, No.(%,N = 393)	200 (50.9)	86 (21.9)[a]	101 (25.7)[a,b]	6 (1.5)
AD, No.(%, N = 126)	22 (17.5)	35 (27.8)[a]	69 (54.8)[a,b]	0 (0.0)
MMSE (N = 750)	28.5 (0.1)	26.9 (0.2)[a]	26.1 (0.2)[a,b]	
ADAS13 (N = 747)	11.6 (0.5)	17.6 (0.7)[a]	21.2 (0.6)[a,b]	
FDG PET SUVR (N = 627)	1.30 (0.01)	1.22 (0.01)[a]	1.18 (0.01)[a,b]	
Hippocampal volume (mm^3) (N = 654)	7268.5 (55.2)	6843.1 (87.0)[a]	6594.0 (74.7)[a]	

Unless otherwise indicated, data are expressed as mean (SD) or N (%)

Statistical analyses were performed with chi-square tests for sex, APOEε4 and diagnosis. Analysis of variance (ANOVA) was used for age and education. Analysis of covariance (ANCOVA) was used for MMSE, ADAS13, FDG PET and hippocampal volumes with covariates of age, sex and education for MMSE, ADAS13 and FDG PET SUVR, plus ICV for hippocampal volumes

Stage 0 means no amyloid involvement in cortical or subcortical regions. Stage 1 means cortical amyloid involvement without subcortical involvement. Stage 2 means amyloid involvement in both cortical and subcortical regions. Unstageable means subcortical amyloid involvement without cortical involvement

[a] $p < 0.05$ between stage 0 and stage 1 or stage 2

[b] $p < 0.05$ between stage 1 and stage 2

Abbreviations: APOEε4, apolipoprotein E ε4 allele; CN, cognitively normal; MCI, mild cognitive impairment; AD, Alzheimer's disease; MMSE, mini-mental state examination; ADAS, Alzheimer's disease assessment scale-cognitive subscale; ICV, intracranial volume